Single cell trapping by capillary pumping using NOA81 replica moulded stencils

Microelectronic Engineering 197 (2018) 1–7

Contents lists available at ScienceDirect

Microelectronic Engineering

journal homepage: www.elsevier.com/locate/mee

Research paper

Single cell trapping by capillary pumping using NOA81 replica moulded stencils

Emma Moonen, Regina Luttge, Jean-Philippe Frimat*

Department of Mechanical Engineering, Microsystems Group and ICMS Institute for Complex Molecular Systems, Eindhoven University of Technology, P.O.Box 513, 5600MB Eindhoven, The Netherlands

ARTICLE INFO

Keywords:
Single cell analysis
NOA81
Replica moulding
Passive pumping
Brain-on-a-chip

ABSTRACT

In this contribution, we demonstrate that the optical adhesive NOA81 (Norland Products Inc.) can be used to replicate optically transparent single cell microsieve structures with exquisite resolution, enabling the fabrication of cheap stencils for single cell trapping applications by the combination of replica moulding and laser micromachining. In addition, we demonstrate an interesting capillary pumping mechanism for gently loading single neuronal cells which eliminates the need for equipment such as pumps and syringes. We demonstrate that capillary pumping through a microsieve generates gentle cell trapping velocities (< 13.3 μm/s), enabling reproducible cell trapping efficiencies of 80% with high cell survival rates (90% over 1 week of culture) and facilitating the formation of spatially standardized neuronal networks.

1. Introduction

Single cell analysis is of paramount importance in biology. That is because cell populations are heterogeneous and their signals tend to be averaged by the general population. Therefore the detection of subpopulations of cells and cellular events at the single cell level within their tissue organization are challenging in every day cell culture. Cell population analysis in bulk: i) blurs cell-to-cell distinctions, ii) makes the detection of rare events leading to disorders and diseases impossible, and iii) does not allow the identification of the individual cell's contribution within a population. For brain research, the gold standard to study these cellular processes are animal models (whole animal or brain slice experiments). Animal models can be useful in elucidating these cellular processes of a fundamental disease's mechanism, but experiments with animal models are slow, have low throughput, are complex, costly, arguably immoral [1] and do not allow single neuron interrogation. In addition, 80% of drugs being successfully studied in animals will fail when applied in humans [2]. Drug screening studies could be improved if relevant human *in vitro* brain models are engineered.

One such route to engineer *in vitro* brain models is microfluidic chip technology. Microfluidics chips are designed for high-throughput and reproducibility, as well as, experimental cost-effectiveness and may be considered to fulfil the demands in pharmacological developments [1,3]. Bringing human physiology onto a chip may more faithfully predict a drug response than existing mouse models [2]. These chips are typically referred to as organ-on-a-chip devices whereby researchers are able to reconstruct the essential function of a human organ [3]. Some examples include liver [4], kidney [5] and lung [6] on-a-chip.

In this research, our goal is to create a chip for a human model of the brain [7] (Fig. 1) to study and better understand epileptic seizures, a model that can also be extended to other investigations of the brain's functioning. Engineering brain tissue on-a-chip, however, is challenging and requires a multidisciplinary approach. The brain is a complex, yet highly organised network of electrically active cells [8]. Neurological disorders and diseases arise when the brain's cellular network is disturbed (*i.e.*, by structural or biochemical damage), which can lead to epilepsy as well as other illnesses such as Alzheimer's, Parkinson's, to name a few. In order to identify and characterise single cell events leading to brain disorders and diseases one must solve the puzzle of competing signals and perform measurements cell by cell (*i.e.*, single-cell analysis).

To date, a large variety of single cell analysis platforms have already been developed [9]. Many have focused on polydimethylsiloxane (PDMS) or glass as the choice of material for a single cell trapping device. We have contributed to this exciting field of BioMEMS often also called cellomics-on-a-chip with the development of a fabrication process for electrically functionalizing microsieves using silicon micromachining. The resulting devices contain highly uniform pyramidal-shaped micropores for the capturing of hundreds of individual neurons in parallel and pairing them onto electrodes [10–12]. This new silicon-based technology platform for multi-site electrophysiology recordings

* Corresponding author.
E-mail address: j.m.s.frimat@tue.nl (J.-P. Frimat).

https://doi.org/10.1016/j.mee.2018.04.010
Received 13 October 2017; Received in revised form 5 April 2018; Accepted 6 April 2018
Available online 07 April 2018

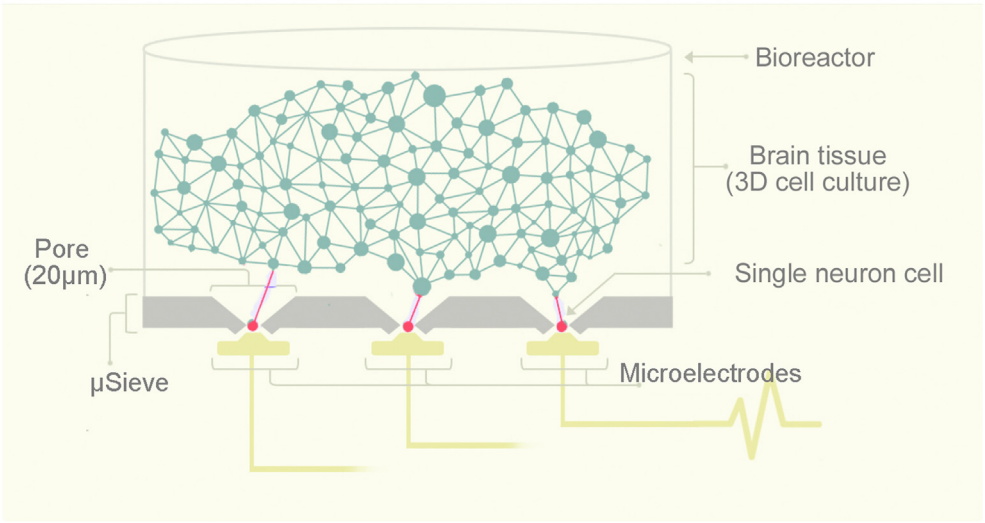

Fig. 1. Schematic representation of the brain-on-a-chip concept. A modified microsieve electrode array (µSEA) with single neurons paired to single electrode is depicted also showing the 3-D brain tissue construct cultured atop the µSEA within a so called bioreactor.

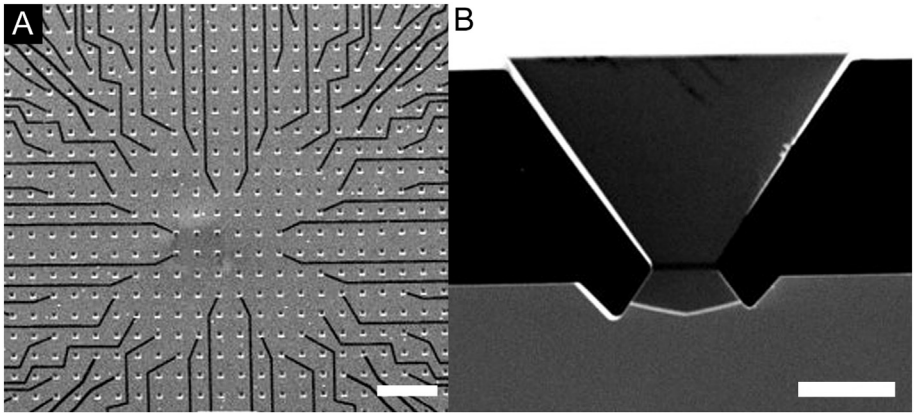

Fig. 2. The microsieve electrode array (µSEA). Overall image of the µSEA with patterned and boron doped poly-silicon (A). The poly-silicon pattern forms the electrode layer consisting of contact electrodes and lead wires (scale bar 200 µm). A cross section of a 3-D micropores with a thickness of approximately 16 µm, top micropore opening of 20 µm and bottom apertures of 3.2 µm (B) (scale bar 5 µm). A more extensive description of the µSEA can be found here [10–12].

was termed MicroSieve Electrode Array (µSEA) (Fig. 2). However, this specific type of platform is still expensive and time consuming to fabricate.

The optical adhesive NOA81 (Norland Products Inc.) is a promising UV-curable alternative material for low-cost microfluidic chip applications [13]. Here, we demonstrate for the first time that the optical adhesive NOA81 can be used to replicate optically transparent microsieve structures with exquisite resolution. This enables the fabrication of cheap stencils for single cell trapping applications by the combination of soft lithography, replica moulding [14] and excimer laser micromachining [15]. This strategy allows to fabricate such type of devices for further evaluation and optimisation of the microfluidic trapping function in cell culture applications. Although we have not yet integrated electrodes in this new polymeric platform, it is of scientific interest to investigate first how such a material can be used in this application.

In this contribution, we describe the new fabrication process for this type of parallel cell trapping microsieve structure. We confirmed an interesting capillary pumping mechanism for gently loading neuronal cells [16] on the microsieve which eliminates the need for additional equipment such as pumps and syringes used in previous microsieve loading protocols [10–12]. We also demonstrated that neurons survive and neuronal networks form on NOA81 microsieves. Finally, we showed for the first time that these uniquely arrayed neurons can be analysed by calcium imaging recordings. Spatially controlled cell patterning for fast, reproducible, parallel mapping of a single neuron's functional behaviour in a dynamically active neuronal network *in vitro* allows us to identify the contribution of a single neuron's activity to the overall network function.

2. Materials and methods

2.1. MicroSieve electrode arrays (µSEA) and soft-lithography template

The MicroSieve Electrode Array (µSEA) used in this study is the original silicon single-cell trapping platform with electrodes and insulation layers developed by Schurink et al. [17] The silicon µSEA design has an array of 900 pyramid-shaped micropores for the hydrodynamic trapping of single cells. These 3D-micropores have a square top opening of 20 µm and a square aperture size at the bottom of 3.2 µm (Fig. 2B). The pores are evenly distributed in a circular area with a radius of 1.2 mm with a pitch of 70 µm. Furthermore, it has integrated contact and sensing electrodes for the recording and stimulation of trapped cells. The full description of its fabrication process has been given by us elsewhere [10–12]. In brief, the fabrication process of the silicon sieving structure is performed by a dedicated set of MEMS processes including anisotropic wet-etching and corner lithography. Subsequently, a patterned boron doped poly-silicon connects the contact electrodes with the sensing electrodes in the pyramid-shaped micropores. A LPCVD silicon-rich silicon nitride layer was used as insulation. In this work, here, we use an original µSEA as a template for soft-lithography.

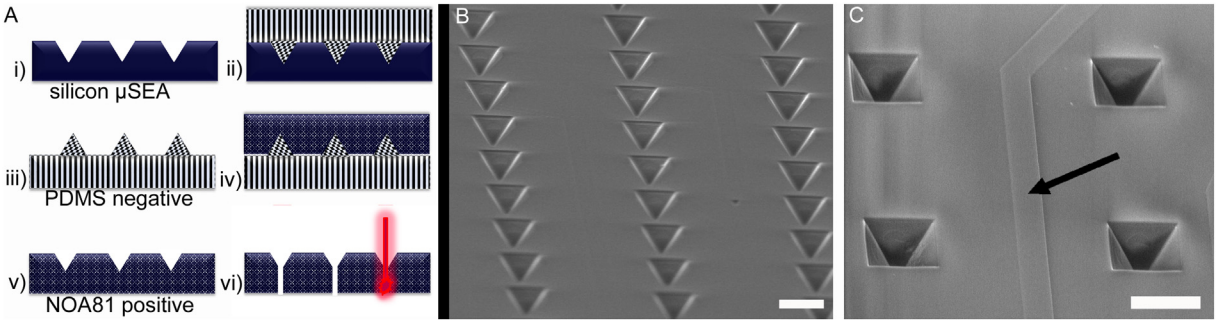

Fig. 3. Dual replication process of the silicon electrode microsieve array (μSEA) into NOA81 (A, *i–vi*). A first negative replica is created by casting PDMS (10/1 w/w ratio) on the μSEA, curing at 95 °C and peeling off (*i–iii*). A drop of NOA81 is applied on the PDMS negative copy (*iv*), and cured using UV for an hour prior to peeling off (*v*). An excitation laser treatment is then applied to open up the pyramid structures and realize the sieve (*vi*). Image showing the negative PDMS (B) and positive NOA81 (C) replica microsieve surfaces (scale bars = 20 μm). Note that the arrow in C shows that features with 220 nm height are faithfully replicated.

2.2. Replica moulding of silicon microsieves in NOA81

In order to replicate the μSEA micropores topography we have used a double replication protocol. The original silicon μSEA was replicated in Polydimethylsiloxane (PDMS) (negative copy) and the PDMS copy was subsequently replicated using NOA81 (positive copy) and cured under UV (emitting 365 nm for an hour). Fig. 3A shows a schematic overview of the steps which are taken into the total replication process. During steps *i* and *ii* a negative replica of the silicon μSEA using PDMS is made. PDMS is a polymer widely used for the fabrication and prototyping of microfluidic chips by replica moulding [18] and has a high replication resolution of up to 50 nm [15]. PDMS and a cross linking agent were mixed in a cup in a ratio of 10:1 and degassed for approximately 20 min. After degassing, the liquid PDMS is poured onto the silicon μSEA (step *ii*) directly from the cup. The layer of PDMS was approximately 400 μm thick. Thereafter, the μSEA/PDMS was cured on a hotplate at 95C° for 10 min and the PDMS was gently peeled off from the μSEA (step *iii*). Step *iv* describes the replication of the structured PDMS negative replica into the positive replica in NOA81. NOA81 is a liquid adhesive that cures to a hard polymer after exposure to UV-light [19]. NOA81 is supplied in a bottle with a special tip for dispensing small droplets. A droplet of NOA81 is put onto the negative PDMS replica and is spread out between the negative PDMS replica and a flat piece of PDMS of about 500 μm thick. After 1 h of UV-curing with a wavelength of 365 nm, the positive NOA81 replica has become rigid and can be easily peeled off from the PDMS. The size of the positive replica is around 1 by 1 cm in area with thickness of 60–110 μm, depending on the size of the flat piece of PDMS and the size of the NOA81 droplet. The pyramid-shaped microcavities featured in NOA81 are then opened up by laser treatment to create micropores.

2.3. Laser micromachining of NOA81 microsieves

The replicated NOA81 samples were submitted to an Optec MicroMaster laser [20] at our Microfab/lab at Eindhoven University of Technology to create through-holes in the pyramid-shaped cavities (Fig. 3A step *vi*). The laser source used in the MicroMaster is the SP 300i short pulse excimer laser manufactured at ATL Lasertechnik [21]. Ultraviolet light is created with KrF gas, which has a characteristic wavelength of 248 nm. The laser pulse duration has an influence on the ablation quality because it controls the peak power and the thermal conduction to the surrounding work material. The pulse duration is essentially the dictating factor in the ablation mechanism [20]. The used excimer laser has a pulse duration of 5–6 ns which classifies as short pulses. This means that thermal damage should be minimal, but the number of pulses can be high. Using a pulse duration of 5–6 ns and a repetition rate of 150 Hz, 5000 pulses were used to create through-holes in the centre of the pyramid-shaped microcavities. Since this serial machining process is relatively slow only 100 out of the total 900 original micropore-structures of the μSEA design were opened for the purpose of demonstrating the fabrication concept. Following the laser ablation process, the NOA81 samples were exposed to UV with a wavelength of 365 nm for another 1 h to ensure that no uncured NOA81 residues remained inside the micropores.

2.4. Cell culture preparation

The neuroblastoma cell line SH-SY5Y was used to characterise the performance of the NOA81 microsieves. The original cell line was isolated from bone marrow taken from a young human female with neuroblastoma [22]. SH-SY5Y neuroblastomas (typical suspension cell diameter 10–15 μm) were cultured in DMEM/F-12 media (1:1) supplemented with 10% FBS and 1% pen/strep and grown in an incubator at 37C°, 5% CO_2. When 80% cell confluency was reached, trypsin (×1) was used to harvest the cells and centrifuged at 900 rpm for 5 min. A concentration of 200,000 cells/ml was used throughout the trapping experiments. Once the cells are positioned within the micropores, they are left to adhere for 2 h. Following the cell trapping, the cells were exposed to retinoic acid for 3 days at 10 μM in DMEM/F-12 media to differentiate the cells into neurons according to the manufacturer protocol [22]. For staining, the cells were fixed in 4% paraformaldehyde for 1 h at room temperature, and then stained for actin (molecular probes, life technologies, ActinGreen 488 ReadyProbes) for 30 min at room temperature according to the manufacturer protocol. A 1 mL droplet of differentiation media is added making sure to fully cover the culture area. Following 3 days of differentiation, we switched to standard culture medium using 1 mL of DMEM/F-12 medium. Samples were thoroughly washed in PBS prior to imaging (EVOS FL microscope, ThermoFisher). For calcium staining experiments, the Fluo-4 Calcium Imaging kit (molecular probes, life technologies) was used according to the manufacturer's protocol and as described by Xie et al. [23].

2.5. Trapping SH-SY5Y cells by capillary pumping

Here, a capillary pumping approach inspired by passive pumping [24] mechanisms was utilised for the demonstration of cell trapping performance in NOA81 microsieves. First, a 10 μL empty (free of cells) media droplet is placed under the microsieve (bottom drop) and the platform is placed into a clean Petri dish. A 20 μL droplet (top drop) containing the cells is immediately placed on top of the microsieve structures and the platform is positioned under the microscope for video recording. Through the capillary action between the microsieve and the flat surface of the Petri dish, a gentle passive flow is generated from top to bottom and through the micropores, which allows to trap the cells in a spatially organised manner in a regular array of 10 × 10 micropores. This phenomena is influenced by 3 different factors: the capillary force which is influenced by the material wettability, passive pumping due to pressure differences between the two droplets and

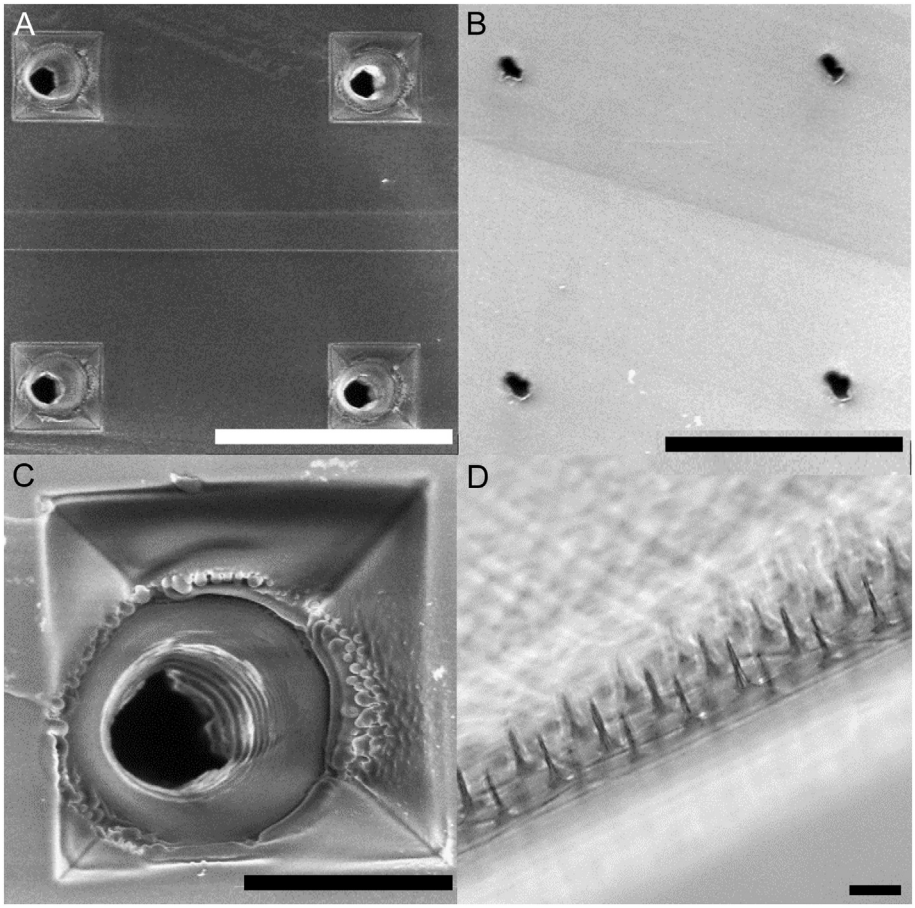

Fig. 4. NOA81 microsieves after the laser treatment. Top and bottom view of a NOA81 microsieve showing four micropores (A–B) (scale bar = 50 μm). Close up of a single micropore (C) (scale bar = 10 μm). Picture showing the final overall NOA81 microsieve platform (D) (scale bar = 50 μm).

gravity which is constant. Taken together, this approach allows the user to seed and trap single neurons without the need for additional equipment such as pumps and syringes as originally designed [11,12]. Thereafter, differentiation medium was applied as described in Section 2.4 above to differentiate the cells but also to remove untrapped cells.

2.6. Neuronal network analysis

For the preliminary neuronal network analysis by calcium imaging we have used a self-made software. The software records the intensity peaks of every single neuron generating a spatio-temporal map of the blinking patterns. When two neuron blink in close proximity and at the same time, the software links them together and assigns the connections.

3. Results and discussion

3.1. NOA81 replication

The optical adhesive NOA81 (Norland Optical Adhesive 81) is a promising UV-curable alternative material for low-cost microfluidic chip applications [13]. NOA81is a single component liquid adhesive that cures in seconds to a tough, hard polymer when exposed to ultraviolet light. It was initially developed as an extremely fast and efficient way to precisely bond optical components or fibre optics [19]. NOA 81 cures to a hard film but it will not become brittle. It has a small amount of resiliency that provides strain relief from vibrations or temperature extremes. This toughness insures long term performance of the material. NOA81 has a viscosity of 300 cps at 25 °C, a 200,000 psi modulus of elasticity and 4000 psi tensile strength [19]. To clarify the need for this replication process, a distinction must be made between the original silicon μSEA and the NOA81 microsieve. The μSEA is the original silicon single-cell trapping platform, with electrodes and insulation layers. The final replicated NOA81 microsieve presented here does not contain the electrodes. It is a topographical copy of the μSEA containing the regular array of 900 geometrically well-defined pyramid-shaped microcavities of which a 10 × 10 array is modified with through-holes by laser micromachining in a serial ablation process to produce the 3D micropores. The latter is performed to produce a sufficient number of microsieve devices for the extensive study of the single cell trapping by capillary pumping, which we previously developed on the original silicon μSEA platform. Different routes for the replication of microstructures from a master exist, the most commonly applied are hot embossing, injection moulding and soft-lithography techniques using polydimethylsiloxane (PDMS). In our experiments we use a double replica moulding procedure with PDMS (negative copy) and NOA81 [19] UV curable polymer (positive copy). The schematic of the double replica moulding procedures is depicted in Fig. 3A (*i–v*) and is described in Section 2.2. The PDMS and NOA81 replicas were imaged after the replication steps and the results are shown in Fig. 3B–C. The pyramid-shaped features in the negative PDMS replica were sharp and all the pyramids were successfully replicated onto the PDMS with high precision (Fig. 3B). Similarly, the replication from PDMS to NOA81 show that all structures were replicated at a very fine detail and that all edges were sharp (Fig. 3C). Furthermore, the square size of the replicated pyramid-shaped microcavities was 20 μm which is the same as the size of the pyramid shaped pores in the original silicon μSEA. This means that accurate pattern transfer of the topography from the

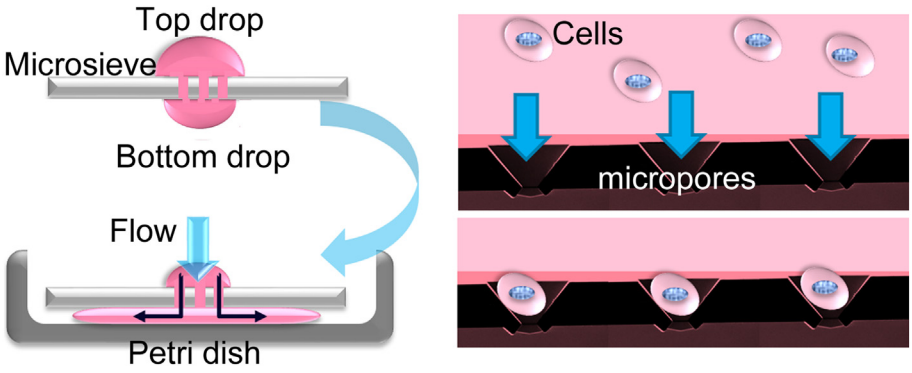

Fig. 5. Schematic representation of the capillary pumping mechanism. A drop is placed atop (top drop) and on the backside (bottom drop) of the microsieve. The microsieve is then placed inside a Petri dish and the bottom drop is flattened between the Petri dish and the microsieve. This action generates a spontaneous capillary pumping effect that initiates a gentle flow from the top drop through the micropores, enabling the trapping of single cells.

template to the NOA81 by means of the intermediate PDMS soft-lithography step was successful. The replication of the thin electrode circuit topography (220 nm in height) in NOA81 was also observed (marked by arrow in Fig. 3C) and is an indication of the high pattern fidelity in our replica moulding protocol (nanometre scale). We chose NOA81 as the material of choice for the second replica step and final microsieve material because it has been also previously characterized for its high replication capability. In addition, this polymer is better suited for making the final positive replica then PDMS because it is more rigid and is therefore easier to manually handle as a cell culture substrate while remaining optically transparent. Also, NOA81 has a weak adhesive affinity to PDMS once UV-cured, meaning that no anti-stiction coating layer has to be applied on the negative PDMS copy.

3.2. Laser micromachining of NOA81

The NOA81 microsieves were made as an array of micropores of 10 by 10. As described in the Materials and Method section the micropores were realized with 5000 pulses and a repetition rate of 150 Hz to produce through-holes with an entrance diameter of approximately 10 µm centrally positioned within the pyramid-shaped microcavities. Fig. 4 shows the resulting laser micromachined NOA81 microsieve. The laser pulse duration has an influence on the ablation quality because it controls the peak power and the thermal conduction to the surrounding work material. The pulse duration is essentially the dictating factor in the ablation mechanism [20]. The lower the pulse duration, the higher the peak power which leads to a more effective ablation process. Long pulses (> 10 ns) can be associated with thermal ablation, which leads to prolonged laser heating and melting and recast of debris. However the removal rate of long pulses is higher, which means that the micropores get deeper with less pulses and thus also less pulses are needed to get through the material. The pulse repetition rate in Hertz is the frequency at which the laser is sending pulses. Pulse repetition rate has very small or no influence on the ablation depth, but it has a noticeable effect on the morphology of the surface [25]. If the rate is too low, all of the energy which was not used for ablation will leave the ablation zone and allows cooling of the ablation zone. If the residual heat can be retained, thus limiting the time for conduction, by a rapid pulse repetition rate, the ablation will be more efficient. Unfortunately, using the current setup at our laboratory, the smallest micropore that could be produced was approximately 10 µm, which is significantly larger than the 3 µm in the original silicon µSEA platform. However, smaller top micropore openings (3–5 µm) would be more desirable as some cells can be smaller than the 10 µm micropores. Even when cells are slightly bigger than 10 µm in diameter they may still simply deform and squeeze through the micropore. The resulting shear forces could even lead to cell membrane rupture and cell death. Nevertheless, since most cells are larger than 10 µm in diameter, we could still use the NOA81 microsieves for the further investigation of the capillary pumping procedure and the optimisation of the cell trapping protocol. Using this replication method consequently also allows us to better understand the influencing parameters in the microfluidic handling procedure of the cell seeding process and to optimise capture conditions for pairing single neurons to micropores when exploiting the full µSEA technology platform including electrodes.

3.3. Capillary pumping and cell trapping

Inspired by early work of Walker and Beebe on passive pumping for microfluidic devices, the utilisation of a simple passive method to drive fluid flow across the pores of the microsieve has been developed. Passive pumping is a simple method for pumping fluids in a semi-autonomous way [24] which eliminates the need for expensive or cumbersome external equipment. In our experiments however, we applied a droplet of fluid (20 µL) on the back of the device and flattened this droplet in between the device and the bottom of a Petri dish. Subsequently the capillary action will continue to generate flow for cell trapping from a cell-laden droplet (10 µL) placed atop of the microsieve (Fig. 5). When this occurs, the weak capillary driven force is directing the flow through the micropores, pulling the top drop in between the microsieve and the Petri dish, initiating a downward flow and enabling the cells to be directed onto the micropores. This can be referred to as capillary pumping. This principle allows gentle flows to be passively generated which are compatible with cell survival (low shear stress) [16]. Initial capillary pumping experiments with 1 µm particles on the original silicon-based µSEA platform indicated that particle trapping speed was on average between 8.6 and 13.3 µm/s depending on the top drop volume [16]. Similarly, capillary pumping for trapping single cells on the NOA81 microsieves generated trapping speeds between 4.4 and 7.1 µm/s (n = 3). The spread in cell trapping velocities is attributed to slight variations of batch to batch NOA81 microsieve fabrication where not all the micropores have exactly the same dimensions (diameter and thickness). However even with these variations, all recorded cell trapping speeds led to successful cell cultures where cell viability remained above 90% following 1 week of culture on the NOA81 microsieves. This was observed by monitoring the trapped neurons ability to spread inside the micropore and develop neurite outgrowth, indicating that these cells did not suffer from the trapping procedure. On average, 1 out of 10 micropores trapped a neuron that did not survive or was already apoptotic when trapped, resulting in the cells never adhering or flattening. Once loaded with neurons, fresh media is added atop the microsieve, washing away untrapped neurons. In addition, the whole trapping procedure is reproducibly achieved within minutes which allows to easily translate such method to a standard biology laboratory. Trapping efficiencies of approximately 80% were achieved in the NOA 81 microsieves (n = 3) (Fig. 6). The efficiency was calculated by dividing the number of filled micropores by the total number of available micropores. This demonstrates the power of a capillary pumping approach for single cell analysis as not only the need for external equipment is eliminated but the flow rates generated are compatible with cell survival.

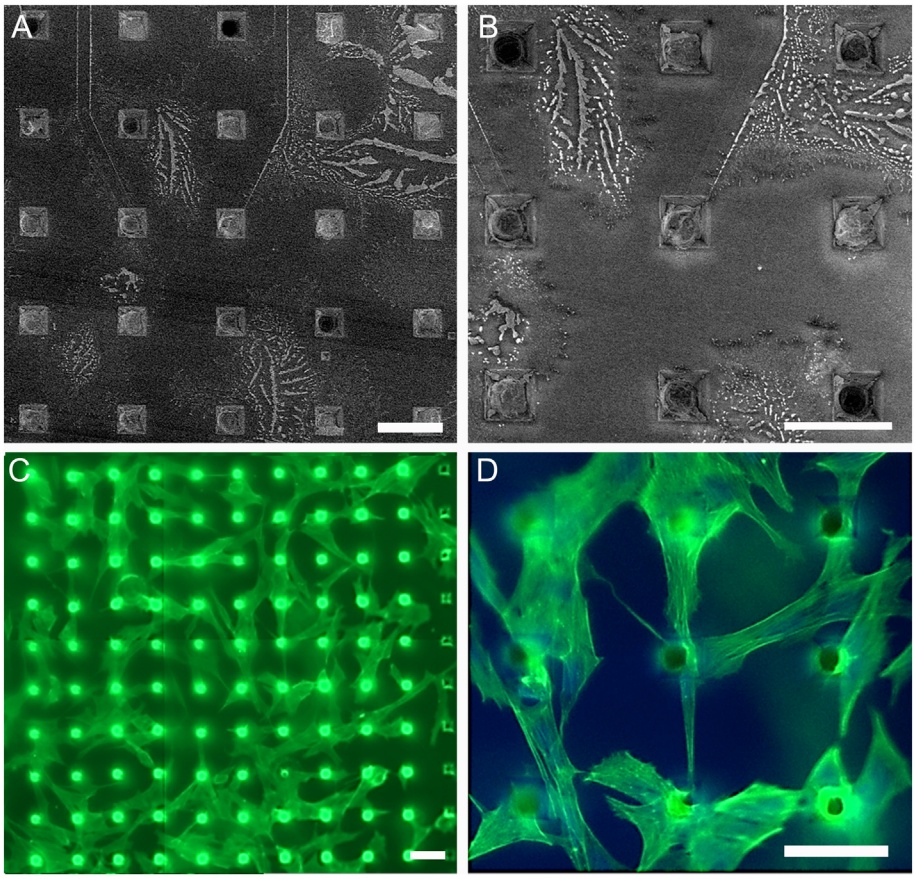

Fig. 6. Result of the trapping of neurons by capillary pumping on NOA81 microsieves. Trapping efficiencies of neurons was typically around 80%, examples with 21 out of 25 (A) and 7 out of 9 (B) single neuron trapped after 3 h of culture. Following 7 days in culture, neurons connected the micropores. An example with 100% filling efficiency is shown (C) as well as a close up of 9 micropores connected by neuron outgrowths (D).

3.4. Analysis of neuronal networks on NOA81 microsieves

Following one week of culture, cells were fixed and stained for actin to highlight spatially patterned neuron interconnectivity. Although not yet perfect, Fig. 6C shows a NOA81 microsieve with 100% trapping efficiency. Neurons formed interconnects from micropore to micropore, with a close up shown in Fig. 6D. Following the successful development of such a cell seeding handling protocol by capillary pumping on NOA81 microsieves, we translate it also to our original silicon-based μSEA. Using the same capillary pumping parameters to trap cells on the micropores, we were able to analyse the arrayed neurons' responses by calcium imaging on the original silicon-based μSEA. Calcium imaging is a technique that highlights active neurons by blinking fluorescent patterns [23]. The fluorescent neuron activity can be recorded into peaks for each neuron and a spatiotemporal map can be generated of active neurons within a network. For example, although these are preliminary results, Fig. 7 show that single neuron activity can be dynamically analysed within an arrayed network and cell to cell networking can be established. This is obtained by comparing the neurons' blinking patterns at fixed locations (trapped neuron) in time (Fig. 7A–B) and identifying which neurons blink in the same time frame, therefore linking them together. In this way, neurons blinking in quick succession and in close proximity can be mapped, as shown in Fig. 7C–D. In Fig. 7C, the size of the dots represent the amount of blinking and time is represented by colour (red to blue). This means that the bigger dots represent neuron with multiple detected peaks (repeated firing) and the colour shows if these neurons are firing in the early (red) or late (blue) time point of the recorded footage. Fig. 7E shows the peak signals detection over time with every detected event represented by a vertical line. When these lines are aligned, synchronous firing is occurring. In future work, NOA81 microsieves and silicon-based μSEA technology should be thoroughly tested with neuronal cells known to be electrically firing such as primary or neuronal stem cells and confirm the compatibility of our procedure with these extremely delicate cells. Thereafter, additional investments may be put into the optimisation of the integration process for electrodes in either of the two platforms (silicon-based μSEA or NOA81 polymer microsieve). This will allow the verification of such an approach to spatially pattern single neurons and identify their behaviour as part of brain functions modelled in the neuronal processes occurring in the arrayed neuronal network. Consequently, brain-on-a-chip technology proposes a coherent set of experiments to provide solutions to a scientific challenging and multi-variant bioengineering problem in tissue engineering, sustaining physiologically relevant cellular cultures, for research in medicine in generally, but specifically with a focus on epilepsy. This neurodynamic disease is characterized by intermittent abnormal synchronisation of different neuronal populations which could be ultimately studied in an arrayed neuronal network.

4. Conclusions

We have used replication and laser micromachining protocols in combination with capillary pumping to optimise the single cell trapping capability of our μSEA platform by removing the need for external equipment such as syringes and pumps. We demonstrate that capillary pumping across a microsieve generates gentle cell trapping velocities ($< 13.3\ \mu m/s$), enabling reproducible cell trapping efficiencies of 80% with high cell survival rates (90% over 1 week of culture) and allowing the formation of spatially standardized neuronal networks. Growing neurons in a spatially standardized fashion (*i.e.*, arrays) will also ease the analysis of neurite connectivity (which is a hallmark neurodevelopmental end point indicator) and will lead to an easier method for relating changes in connectivity to electrophysiology and biological function. Proof of concept experiments on single neuron activity by

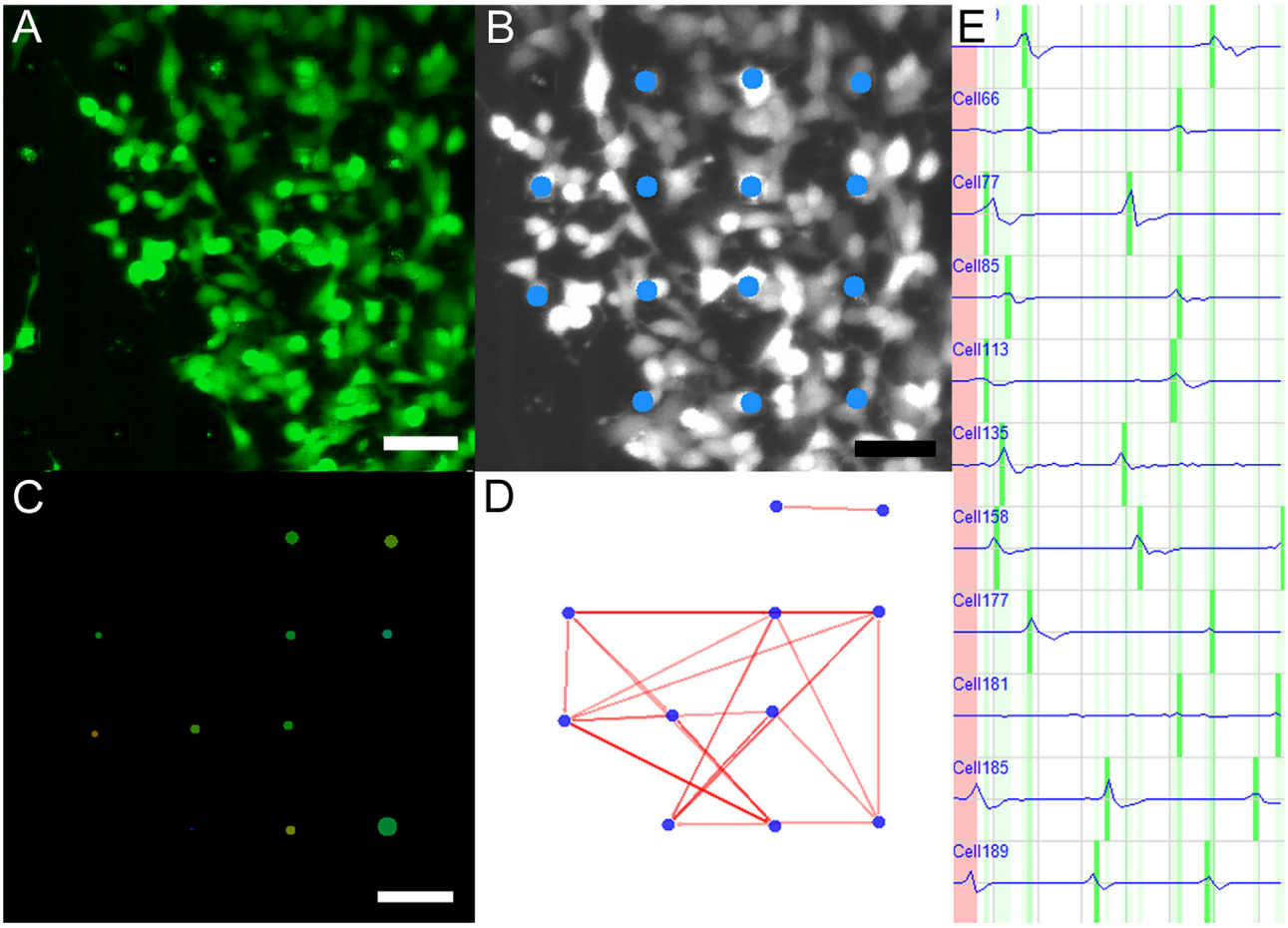

Fig. 7. Calcium imaging of neurons trapped by capillary pumping on the original silicon μSEA. Neurons fluorescently labelled with calcium dye (A) and location of calcium measurements (B). The resulting spatio-temporal map (C). This creates a colour coded map in time (blue to red) with the size of the dots representing the amount of blinking. Neurons blinking in the same time frame are inter-connected (D). Fluorescent peak detection of blinking neurons over time (E). (For interpretation of the references to colour in this figure legend, the reader is referred to the web version of this article.)

calcium imaging is shown, where neuron interconnectivity can be determined and analysed over time, paving the road for dynamic single neuron interrogation within an arrayed neuronal network as a model for distinguished brain functions.

Acknowledgements

This research is financially supported by the ERC grant 280281 (MESOTAS) and the ERC-PoC MESOTAS SIEVE grant 713732. The authors would also like to acknowledge Fer Radstake for his contribution with the development of the calcium imaging software.

References

[1] L.A. Low, D.A. Tagle, Clin. Transl. Sci. 10 (4) (2017) 237–239.
[2] S. Perrin, Nature 507 (7493) (2014) 423–425.
[3] A.D. van der Meer, A. van den Berg, Integr. Biol. 4 (2012) 461.
[4] P.J. Lee, P.J. Hung, L.P. Lee, Biotechnol. Bioeng. 97 (2007) 1340–1346.
[5] L.C. Snouber, F. Letourneur, P. Chafey, C. Broussard, M. Monge, C. Legallais, E. Leclerc, Biotechnol. Prog. 28 (2012) 474–484.
[6] D. Huh, B.D. Matthews, A. Mammoto, M. Montoya-Zavala, H.Y. Hsin, D.E. Ingber, Science 328 (2010) 1662–1668.
[7] J.P. Frimat, S. Xie, A. Bastieans, B. Schurink, F. Wolbers, J. Den Toonder, R. Luttge, J. Vac. Sci. Technol. B 33 (2015) 06F902-6.
[8] O. Sporns, Nat. Neurosci. 17 (2014) 652.
[9] A. Gross, J. Schoendube, S. Zimmermann, M. Steeb, R. Zengerle, P. Koltay, Int. J. Mol. Sci. 16 (2015) 16897–16919.
[10] B. Schurink, R. Luttge, J. Vac. Sci. Technol. B 31 (2013) 06F903.
[11] B. Schurink, J.W. Berenschot, R.M. Tiggelaar, R. Luttge, Microelectron. Eng. 144 (2015) 12.
[12] B. Schurink, R.M. Tiggelaar, J.G.E. Gardeniers, R. Luttge, J. Micromech. Microeng. 27 (2016) 015017.
[13] P. Wägli, A. Homsy, N.F. de Rooij, Procedia Eng. 5 (2010) 460–463.
[14] Y.N. Xia, G.M. Whitesides, Annu. Rev. Mater. Sci. 28 (1998) 153–184.
[15] ATL Lasertechnik GmbH, ATL Lasertechnik Advanced Technology Lasers, (2007).
[16] J.P. Frimat, B. Schurink, R. Luttge, J. Vac. Sci. Technol. B 35 (2017) 06GA01-6.
[17] B. Schurink, Thesis, Faculty of Science and Technology, University of Twente, The Netherlands, Mesoscale Chemical Systems, 2016.
[18] S. Halldorsson, E. Lucumi, R. Gómez-Sjöberg, R.M.T. Fleming, Biosens. Bioelectron. 63 (2015) 218–231.
[19] Norland-Products-Incorporated, Produktinformationen zu NORLAND PRODUCTS IN-CORPORATED Norland Optical Adhesive, 81 (1966), pp. 1–2.
[20] S.A. Optec, MicroMaster User Instruction Manual. Frameries, Belgium, 6.6 edition, (2005).
[21] Y. van de Burgt, Y. Bellouard, R. Mandamparambil, Kinetics of Laser-Assisted Carbon Nanotube Growth, Phys. Chem. Chem. Phys. (2014), http://dx.doi.org/10.1039/C4CP00061G.
[22] SIB Swiss Institute of Bioinformatics. Cellosaurus SH-SY5Y (CVCL 0019).
[23] S. Xie, J.G.E. Gardeniers, R. Luttge, MicroTAS, 20th International Conference on Miniaturized Systems for Chemistry and Life Sciences, 2016, pp. 495–496.
[24] G.M. Walker, D.J. Beebe, Lab on Chip, 2 (2002), pp. 131–134.
[25] S. Magadum, M. Chellamalai, N. Balashanmugam, Adv. Nanosci. Technol. 1 (2) (2015) 1–6.